

LATTICE QCD THERMODYNAMICS*

Z. FODOR^{a,b}, S.D. KATZ^b^aUniversity of Wuppertal, Gausstrasse 20, 42119 Wuppertal, Germany^bEotvos University, Egyetem tér 1–3, 1053 Budapest, Hungary*(Received November 8, 2011)*

In this paper, the basics of finite temperature lattice QCD are summarised. At high temperatures there is a transition from a state dominated by colourless hadrons to a state dominated by coloured particles. The nature of this transition is determined to be an analytic cross-over. The absolute scale (the transition temperature T_c) is calculated for various observables. Finally, the equation of state of the strongly interacting matter is presented.

DOI:10.5506/APhysPolB.42.2791

PACS numbers: 11.15.Ha, 12.38.Gc, 11.10.Wx, 12.38.Mh

1. Introduction

The theory of the strong interaction is quantum chromo-dynamics (QCD). The Lagrangian of QCD contains only quarks and gluons, which are unobservable in experiments. Instead of free quarks and gluons we observe bound state hadrons. The perhaps most important feature of QCD is asymptotic freedom. At small energies the interaction is strong, the value of the coupling constant is large. For large energies the coupling constant decreases and approaches zero, which means that the particles are interacting less and less. Since the coupling constant is large at small energies, we cannot use one of the most powerful methods of particle physics, the perturbative approach.

At small energies (below about 1 GeV) the bound states and their interactions can be described only by non-perturbative methods. The most systematic non-perturbative technique today is lattice field theory. The field variables of the Lagrangian are defined on a discrete space-time lattice. The continuum results are obtained by taking smaller and smaller lattice spacings (a) and extrapolating the results to vanishing a . Though lattice field theory has been an active field for about 35 years, the first continuum extrapolated full results appeared only recently.

* Presented at the LI Cracow School of Theoretical Physics “Soft Side of the LHC”, Zakopane, Poland, June 11–19, 2011.

A consequence of asymptotic freedom is that the coupling decreases for high temperatures (they are also characterised by large energies). According to the expectations at very high temperatures (Stefan–Boltzmann limit) the typical degrees of freedom are no longer bound state hadrons but freely moving quarks and gluons. Since there are obvious qualitative differences between these two forms of matter, we expect a phase transition between them at a given temperature T_c . The value of T_c can be estimated to be the typical QCD scale (≈ 200 MeV).

In this paper, the QCD transition at non-vanishing temperatures will be studied. We will use lattice gauge theory to give non-perturbative predictions. First, the phase diagram at vanishing chemical potential is discussed. In the next section, we summarise the necessary techniques of lattice gauge theory. After that, we determine the nature of the transition (first order, second order or analytic crossover) and the characteristic scale of the transition (we call it transition temperature T_c). According to the detailed analyses there is no singular phase transition in the system, instead, one is faced with an analytic — crossover like — transition between the phases dominated by quarks/gluons and that with hadrons (from now on we call these two different forms of matter phases). As a consequence, there is no unique transition temperature. Different quantities give different T_c values (which are then defined as the most singular point of their temperature dependence). We will determine the equation of state as a function of the temperature, too.

2. The phase diagram of QCD

Before we discuss the results, let us summarise the qualitative picture of the QCD phase diagram. Figure 1 shows the conjectured phase diagram of QCD as a hypothetical function of the m_{ud} light quark mass and m_s strange quark mass. In nature, these quark masses are fixed and they correspond to a single point on this phase diagram. The figure shows our expectations for the nature of the transition. QCD is a gauge theory, which has two limiting cases with additional symmetries. One of these limiting cases correspond to the infinitely heavy quark masses (point D of the diagram). This is the pure SU(3) Yang–Mills theory, which has not only the SU(3) gauge symmetry but an additional Z(3) center symmetry, too. At high temperatures this Z(3) symmetry is spontaneously broken. The order parameter which belongs to the symmetry is the Polyakov loop. The physical phenomenon, which is related to the spontaneous symmetry breaking is the deconfining phase transition. At high temperatures the confining feature of the static potential disappears. The first lattice studies were carried out in the pure SU(2) gauge theory [1,2]. The transition turned out to be a second order phase transition. Later on the increase of the computational resources allowed to study the

SU(3) Yang–Mills theory. It was realized that in this case we are faced with a first order phase transition, which happens around 270 MeV in physical units [3, 4, 5, 6, 7].

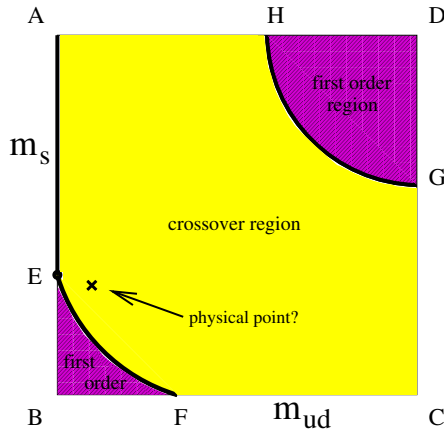


Fig. 1. The conjectured phase diagram of QCD on the hypothetical m_s – m_{ud} plane (strange quark mass *versus* light — up and down — quark mass, from now on we use degenerate light quark masses). The middle region corresponds to analytic crossover. In the lower left and upper right (purple) regions one expects a first order phase transition. On the boundaries between the first order phase transition regions and the crossover region and along the AE line the transition is of second order.

The other important limiting case corresponds to vanishing quark masses (points A and B). In this case the Lagrangian has an additional global symmetry, namely chiral symmetry. Left and right handed quarks are transformed independently. Point A corresponds to a two flavour theory ($N_f = 2$), whereas the three flavour theory ($N_f = 3$) is represented by point B. The chiral symmetry can be described by $U(N_f)_L \times U(N_f)_R$. At vanishing temperature the chiral symmetry is spontaneously broken, the corresponding Goldstone bosons are the pseudoscalar mesons (in the $N_f = 2$ case we have three pions). Since in nature the quark masses are small but non-vanishing the chiral symmetry is only an approximative symmetry of the theory. Thus, the masses of the pions are small but non-zero (though they are much smaller than the masses of other hadrons; for a full calculation within the lattice framework see [8]). At high temperatures the chiral symmetry is restored. There is a phase transition between the low temperature chirally broken and the high temperature chirally symmetric phases. The corresponding order parameter is the chiral condensate. For this limiting case we do not have reliable lattice results (lattice simulations are prohibitively expensive for small quark masses, thus to reach the zero

mass limit is extremely difficult). There are model studies, which start from the underlying symmetries of the theory. These studies predict a second order phase transition for the $N_f = 2$ case, which belongs to the $O(4)$ universality class. For the $N_f = 3$ theory these studies predict a first order phase transition [9]. For intermediate quark masses we expect an analytic crossover (see Fig. 1). One of the most important questions is to locate the physical point on this phase diagram, thus to determine the nature of the $T > 0$ QCD transition for physical quark masses.

The determination of the phase diagram for non-vanishing chemical potentials by dynamical lattice simulations (initiated by [10, 11]) will be not discussed here. The interested reader can consult the review [12] or some original papers (*e.g.* the first physical quark mass result [13] or the first one with an additional continuum limit extrapolation [14]).

3. QCD thermodynamics on the lattice

We summarise the most important ingredients of lattice QCD. Instead of providing a complete introduction we focus on those elements of the theory and techniques, which are essential to lattice thermodynamics. A detailed introduction to other fields of lattice QCD can be found in Ref. [15].

Thermodynamic observables are derived from the grand canonical partition function. The Euclidean partition function can be given by the following functional integral

$$Z = \int \mathcal{D}U \mathcal{D}\bar{\psi} \mathcal{D}\psi e^{-S_E(U, \bar{\psi}, \psi)}. \quad (1)$$

Here U represent the gauge fields (gluons), whereas ψ and $\bar{\psi}$ are the fermionic fields (quarks). QCD is an $SU(3)$ gauge theory with fermions in the fundamental representation. Thus, at various space-time points the four components of the U gauge field can be given by $SU(3)$ matrices for all four directions. The fermions are represented by non-commuting Grassmann variables.

The Boltzmann factor is given by the Euclidean action, which is a functional of the gauge and fermionic fields. Equation (1) contains additional parameters (though they are not shown in the formula explicitly). These parameters are the β gauge coupling (it is related to the continuum gauge coupling as $\beta = 6/g^2$) and the quark masses (m_i). For simplicity, Eq. (1) describes only one flavour. More than one flavour can be described by introducing several ψ_i fields. In nature there are six quark flavours. The three heaviest flavours (c, b, t) are much heavier than the typical energy scales in our problem. They do not appear as initial or final states and they cannot be produced at the typical energy scales. Their effects can be included by

a simple redefinition of the other bare parameters (for some quantities they should be included explicitly as dynamical degrees of freedom). The three other quarks are the u , d and s quarks. The masses of the u , d quarks are much smaller than the typical hadronic scale, therefore one can treat them as degenerate degrees of freedom (exact SU(2) symmetry is assumed). This approximation is satisfactory, since the mass difference between the u and d quarks can explain only $\approx 50\%$ of the mass difference between different pions. For the remaining $\approx 50\%$ the electromagnetic interaction is responsible (the up and down quarks have different electric charges). Including the mass differences would mean that one should include an equally important feature of nature, namely the electromagnetic interactions, too. This is usually far beyond the precision lattice calculations can reach today. Assuming $m_u = m_d$ is a very good approximation, the obtained results are quite precise, uncertainty related to this choice is clearly subdominant. For the degenerate up and down quark mass we use the shorthand notation m_{ud} . The s quark is somewhat heavier, its mass is around the scale of the Λ parameter of QCD. In typical lattice applications one uses the $m_u = m_d < m_s$ setup, which is usually called as $N_f = 2 + 1$ flavour QCD.

In order to give the integration measure $(DU\mathcal{D}\psi\mathcal{D}\bar{\psi})$, one has to regularise the theory. Instead of using the continuum formulation we introduce a hypercubic space-time lattice Λ . The fields are defined on the sites (fermions) and on the links (gauge fields) of this lattice. It is easy to show that this choice automatically respects gauge invariance. For a given site $x \in \Lambda$ four $(x; \mu)$ links can be defined (here μ denotes the direction of the link, $\mu = 1 \dots 4$). Using this choice the integration measure is given by

$$DU\mathcal{D}\bar{\psi}\mathcal{D}\psi = \prod_{x \in \Lambda, \mu=1 \dots 4} dU_{x;\mu} \prod_{x \in \Lambda} d\psi_x \prod_{x \in \Lambda} d\bar{\psi}_x. \quad (2)$$

With this regularisation one can imagine the functional integral as a sum of the Boltzmann factors $\exp(-E/kT)$ over all possible $\{U, \psi, \bar{\psi}\}$ configurations (here we use the $k = 1$ convention). Thus, our system corresponds to a four-dimensional classical statistical system. The energy functional is simply replaced by the Euclidean action. An important difference is that in statistical physics the temperature is included in the Boltzmann factor, whereas in our case it is related to the temporal extent of the lattice (it is the inverse of it). It is easy to show that using periodic boundary conditions for the bosonic fields and antiperiodic boundary conditions for the fermionic fields our Eq. (1) reproduces the statistical physics partition function.

3.1. The action in lattice QCD

The lattice regularisation means that one should discretise the Euclidean action S_E . This step is not unambiguous. There are several lattice actions, which all lead to the same continuum action. The difference between them is important, since these differences tell us how fast they approach the continuum result as we decrease the lattice spacing. Calculating a given A observable on the lattice of a lattice spacing a , the result differs from the continuum one

$$\langle A \rangle_a = \langle A \rangle + \mathcal{O}(a^\eta) . \quad (3)$$

The power η depends on the way we discretised the action. The larger the power η the better the action (for large η we can obtain a result, which is quite close to the continuum one, already at large lattice spacing).

The most straightforward discretisation is obtained by simply taking differences at neighbouring sites to approximate derivatives. Actions, which have better scaling behaviour (larger η or smaller prefactor) are called improved actions.

In the following paragraphs we summarise the most important actions.

The action S_E usually can be written as a sum $S_E = S_g + S_f$, where S_g is the gauge action (it depends only on the gauge fields) and S_f is the fermionic action (it depends both on the gauge and fermionic fields).

The simplest gauge action is the Wilson gauge action which is the sum of the

$$U_P(x; \mu\nu) = U_{x;\mu} U_{x+a\hat{\mu};\nu} U_{x+a\hat{\nu};\mu}^\dagger U_{x;\nu}^\dagger \quad (4)$$

plaquettes. Here $\hat{\mu}$ denotes the unit vector in the μ direction. The Wilson action reads

$$S_{g,\text{Wilson}} = -\beta \left(\frac{1}{3} \sum_{x,\mu<\nu} \text{Re Tr } U_P(x; \mu\nu) - 1 \right) . \quad (5)$$

This action is the simplest real, gauge invariant expression, which can be constructed using the gauge fields. One can show, that in the continuum limit the above expression leads to the usual Yang–Mills gauge action.

One can improve the action by adding other gauge invariant terms. The simplest such improvement term is provided by the 2×1 rectangles, for which — analogously to the plaquette term — we multiply the $SU(3)$ link matrices around the rectangle. Denoting this term by $U_{2 \times 1}(x; \mu\nu)$ one obtains the following action

$$S_g = -\frac{\beta}{3} \left(c_0 \sum_{x,\mu<\nu} \text{Re Tr } U_P(x; \mu\nu) + c_1 \sum_{x,\mu \neq \nu} \text{Re Tr } U_{2 \times 1}(x; \mu\nu) \right) . \quad (6)$$

It can be shown that this choice improves the scaling. On the tree level the condition $c_0 + 8c_1 = 1$ should be fulfilled and $c_1 = -1/12$. This is the (tree level improved) Symanzik gauge action. Other improvements use also chair-like closed paths and non-perturbative coefficients. Note, however, that the tree level improvement is usually enough for thermodynamic studies, the main source of difficulties is in the fermionic part (further improvements in the gauge sector can be considered as a sort of “over-killing”).

Discretising the fermionic fields is more difficult than discretising gauge fields. The naive discretisation leads to the following action

$$S_{f,naive} = \sum_x \left[am\bar{\psi}\psi + \frac{1}{2} \sum_{\mu=1\dots4} \left(\bar{\psi}_x U_{x;\mu} \gamma_\mu \psi_{x+a\hat{\mu}} - \bar{\psi}_x U_{x-a\hat{\mu};\mu}^\dagger \gamma_\mu \psi_{x-a\hat{\mu}} \right) \right] \quad (7)$$

in the free case ($U = 1$) the propagator has 16 poles in the Brillouin zone (we expected only one). Thus, contrary to the continuum case our lattice action describes 16 degenerate fermions instead of 1 fermion.

There are several ways to resolve this problem. The two most popular solutions are the Wilson and the Kogut–Susskind regularisations. The problem is related to the fact that the continuum fermion action contains only first derivatives. The basic idea of the Wilson fix is to add a second derivative term — Wilson term — to the action: $a\bar{\psi}\partial_\mu\partial_\mu\psi$. This term vanishes in the continuum limit. For non-vanishing lattice spacings the Wilson term increases the masses of the 15 non-physical modes so that they are at the cutoff scale ($1/a$). As we approach the continuum limit these 15 particles decouple. Generally, one can use a Wilson term with an arbitrary coefficient r . The usual choice is $r = 1$. In this case the action reads

$$S_{f,Wilson} = \sum_x \left[\bar{\psi}\psi + \kappa \sum_{\mu=1\dots4} \left(\bar{\psi}_x U_{x;\mu} (1+\gamma_\mu) \psi_{x+a\hat{\mu}} + \bar{\psi}_x U_{x-a\hat{\mu};\mu}^\dagger (1-\gamma_\mu) \psi_{x-a\hat{\mu}} \right) \right]. \quad (8)$$

Here the fields are rescaled appropriately. The disadvantage of Wilson fermions is the loss of chiral symmetry for vanishing quark masses. This symmetry is restored only in the continuum limit. The quark mass receives an additive renormalisation and the asymptotic scaling (*cf.* Eq. (3)) is linear in a .

Kogut and Susskind introduced another formalism, namely the *staggered* fermions. The spinor components of the fermionic field are distributed among the corners of a 2^4 hypercube. This leads to a diagonal expression in the spinor index. By using only 1 out these 4 diagonal components one can reduce the number of degrees of freedom by a factor of 4. This action

describes $16/4 = 4$ fermions of the same mass. The action can be written as

$$S_{\text{f, staggered}} = \sum_x \left[am \bar{\chi} \chi + \frac{1}{2} \sum_{\mu=1 \dots 4} \alpha_{x;\mu} \left(\bar{\chi}_x U_{x;\mu} \chi_{x+a\hat{\mu}} - \bar{\chi}_x U_{x-a\hat{\mu};\mu}^\dagger \chi_{x-a\hat{\mu}} \right) \right], \quad (9)$$

where $\alpha_{x;\mu} = (-1)^{x_1 + \dots + x_{\mu-1}}$. Contrary to the naive or Wilson fermion formulations, the χ field has only one spin component. For simplicity, we use the Greek letter ψ also for staggered fermions. The most important advantage of the staggered formalism is, that the action has a $U(1)_{\text{L}} \times U(1)_{\text{R}}$ symmetry (which is a remnant of the original chiral symmetry). Due to this symmetry there is no additive mass renormalisation. The asymptotic scaling is better than for Wilson fermions, it is proportional to a^2 . An additional advantage is of computational nature. Since we do not have Dirac indices the computations are faster. The most important disadvantage of the staggered fermions is the fourfold degeneracy of the fermions. Later we discuss the technique, which allows one to use less than four fermions.

There are two other fermion formulations (overlap and domain-wall) with very attractive theoretical features. Note, however, that they are numerically so expensive and did not provide yet full thermodynamical results.

Both equations (8) and (9) are bilinear in the fermionic fields (it is true for other actions, too)

$$S_{\text{f}} = \sum_{x,y} \bar{\psi}_x M_{xy}(U) \psi_y, \quad (10)$$

here the specific form of the matrix M can be derived from Eqs. (8) and (9). It means that the fermionic integrals can be evaluated exactly. Using the known Grassmann integration rules one obtains

$$\int \mathcal{D}\bar{\psi} \mathcal{D}\psi e^{-S_{\text{f}}} = \det M(U). \quad (11)$$

Thus the partition function (1) can be written as follows

$$Z = \int \mathcal{D}U \det M(U) e^{-S_{\text{g}}(U)} = \int \mathcal{D}U e^{-\{S_{\text{g}}(U) - \ln \det M\}}. \quad (12)$$

This simple step resulted in an effective theory, which contains only bosonic fields. The action reads: $S_{\text{eff.}} = S_{\text{g}} - \ln \det M$. Unfortunately, this action is non-local. Due to the fermionic determinant fields at arbitrary distances interact with each other (the original action $S_{\text{E}} = S_{\text{g}} + S_{\text{f}}$ is local in the field variables). This non-locality is the most important source of difficulties. It

is much more demanding to study full QCD (with dynamical fermions) than pure SU(3) gauge theory.

In the rest of this work, we will deal with staggered theory, only. Since staggered fermions are computationally less demanding than other fermion formulations, the vast majority of the results in the literature are obtained by using staggered fermions. Another reason why the staggered fermions are so popular for thermodynamic studies is related to the fact that staggered fermions are invariant under (reduced) chiral symmetry, which might play an important role for questions such as chiral symmetry restoration (at the finite temperature QCD transition).

In numerical simulations we use finite size lattices of $N_s^3 N_t$. The three spatial sizes are usually the same (N_s), they give the spacial volume of the system, whereas the temporal extension in Euclidean space-time is directly related to the temperature

$$V = (N_s a)^3, \quad T = \frac{1}{N_t a}. \quad (13)$$

Lattices with $N_t \geq N_s$ are called “zero temperature” lattices, and lattices with $N_t \ll N_s$ are called “non-zero temperature” lattices. In thermodynamic studies a small temperature region around the transition temperature is the main focus of the analyses (an exception is the determination of the equation of state, which can be studied at much higher temperatures, too). According to $T = 1/(N_t a)$ one can fix the temperature by using smaller and smaller lattice spacings and larger and larger N_t temporal extensions. Thus, the resolution of an analysis is usually characterised by the temporal extension. In the literature, one finds typically N_t values of 4, 6, 8, 10, 12 and 16, which correspond to lattice spacings (at and around T_c) of approximately $a = 0.3, 0.2, 0.15, 0.12, 0.1$ and about 0.07 fm, respectively. We give here only approximative values and it is impossible to give precise values for the lattice spacings, particularly for the relatively coarse lattices. The reason for this “no-go” observation can be summarised as follows. QCD predicts only dimensionless combinations of observables. These combinations are only approximated on the lattices, they have a^n scaling corrections, which vanish as we approach the continuum limit. Since different combinations have different scaling corrections, the lattice spacing cannot be given unambiguously.

3.2. Continuum limit

The final goal of lattice QCD is to give physical answers in the continuum limit. Results at various lattice spacings, a , are considered as intermediate steps. Since the regularisation (lattice) is inherently related to the non-vanishing lattice spacing it is not possible to carry out calculations already

in the continuum limit in our lattice framework. The continuum physics appears as a limiting result. Obviously, the $a \rightarrow 0$ limit should be carried out according to Eq. (3). During this procedure the physical observables, more precisely their dimensionless combinations should converge to finite values. On the way to the continuum limit one should tune the parameters of the Lagrangian as a function of the lattice spacing. The renormalisation group equations tell us how the parameters of the Lagrangian depend on the lattice spacing. For small gauge coupling (thus, for large cutoff or close to the continuum limit) the perturbative form of the renormalisation group equations can be used. For somewhat larger gauge couplings one should use non-perturbative relationships.

Usually, when one changes the lattice spacing (*e.g.* all the way to the continuum limit) the form of the action remains the same, only its parameters are changed. The way the parameters change is called renormalisation group flow or line of constant physics (LCP). It can be obtained by choosing a few dimensionless combinations of observables and demanding that their values remain the same “predefined” value as we change the lattice spacing. Using different sets of observables result in different LCPs; however, these different LCPs merge when we approach the continuum limit. The LCPs are usually determined by non-perturbative techniques. The simplest procedure is to measure the necessary dimensionless combinations at various parameters of the action (bare parameters) and interpolate to those bare parameters, at which the dimensionless combinations take their predefined value. A few iterative steps are usually enough to reach the necessary accuracy.

4. The nature of the transition

As we will see the nature of the transition is a cross-over. This is a highly non-trivial result obtained with physical quark masses extrapolated to the continuum limit and performing a finite volume analysis. This result affects our understanding of the universe’s evolution (see *e.g.* Ref. [16]). In a strong first order phase transition scenario the quark-gluon plasma super-cools before bubbles of hadron gas are formed. These bubbles grow, collide and merge during which gravitational waves could be produced [17]. Baryon enriched nuggets could remain between the bubbles contributing to dark matter. Since the hadronic phase is the initial condition for nucleosynthesis, the above picture with inhomogeneities could have a strong effect on it [18]. As the first order phase transition weakens, these effects become less pronounced. Recent calculations provide strong evidence that the QCD transition is an analytic transition (what we call here a crossover), thus the above scenarios — and many others — are ruled out.

In order to determine the nature of the transition, one should apply finite size scaling techniques for the chiral susceptibility [19]. $\chi = (T/V) \times (\partial^2 \log Z / \partial m_{ud}^2)$. This quantity shows a pronounced peak as a function of the temperature. For a first order phase transition, such as in the pure gauge theory, the peak of the analogous Polyakov susceptibility gets more and more singular as we increase the volume (V). A second order transition shows a similar singular behaviour with critical indices. For an analytic transition (crossover) the peak width and height saturates to a constant value.

One can carry out a finite size scaling analysis with the continuum extrapolated height of the renormalised susceptibility. The renormalisation of the chiral susceptibility can be done by taking the second derivative of the free energy density (f) with respect to the renormalised mass (m_r). The logarithm of the partition function contains quartic divergences. These can be removed by subtracting the free energy at $T = 0$: $f/T^4 = -N_t^4 [\log Z(N_s, N_t)/(N_t N_s^3) - \log Z(N_{s0}, N_{t0})/(N_{t0} N_{s0}^3)]$. This quantity has a correct continuum limit. The subtraction term is obtained at $T = 0$, for which simulations are carried out on lattices with N_{s0}, N_{t0} spatial and temporal extensions (otherwise at the same parameters of the action). The bare light quark mass (m_{ud}) is related to m_r by the mass renormalisation constant $m_r = Z_m \cdot m_{ud}$. Note that Z_m falls out of the combination $m_r^2 \partial^2 / \partial m_r^2 = m_{ud}^2 \partial^2 / \partial m_{ud}^2$. Thus, $m_{ud}^2 [\chi(N_s, N_t) - \chi(N_{s0}, N_{t0})]$ also has a continuum limit (for its maximum values for different N_t , and in the continuum limit we use the shorthand notation $m^2 \Delta\chi$).

In order to carry out the finite volume scaling in the continuum limit, three different physical volumes were taken. For these volumes the dimensionless combination $T^4/m^2 \Delta\chi$ was calculated at 4 different lattice spacings: 0.3 fm was always off, otherwise the continuum extrapolations could be carried out. Figure 2 shows these extrapolations. The volume dependence of the continuum extrapolated inverse susceptibilities is shown in Fig. 3.

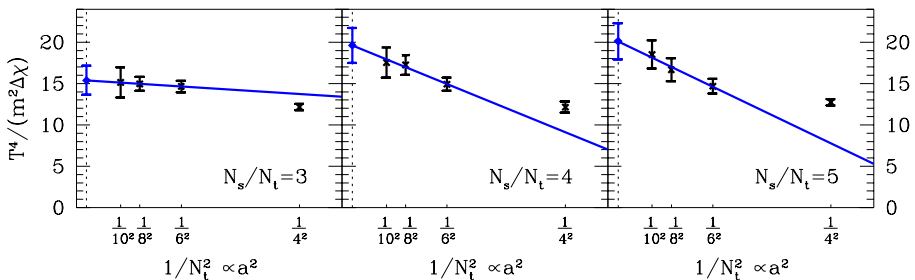


Fig. 2. Normalized susceptibilities $T^4/(m^2 \Delta\chi)$ for the light quarks for aspect ratios $r = 3$ (left panel) $r = 4$ (middle panel) and $r = 5$ (right panel) as functions of the lattice spacing. Continuum extrapolations are carried out for all three physical volumes and the results are given by the leftmost blue diamonds.

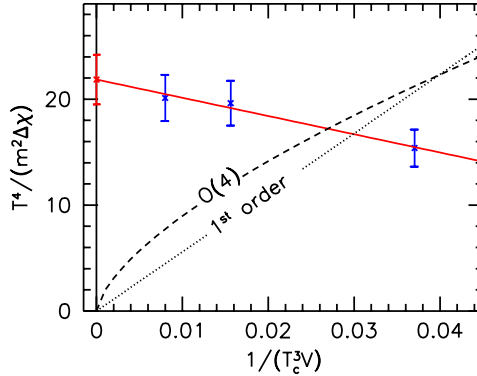


Fig. 3. Continuum extrapolated susceptibilities $T^4/(m^2\Delta\chi)$ as a function of $1/(T_c^3V)$. For true phase transitions the infinite volume extrapolation should be consistent with zero, whereas for an analytic crossover the infinite volume extrapolation gives a non-vanishing value. The continuum-extrapolated susceptibilities show no phase-transition-like volume dependence, though the volume changes by a factor of five. The $V \rightarrow \infty$ extrapolated value is 22(2) which is 11σ away from zero. For illustration, we fit the expected asymptotic behaviour for first-order and $O(4)$ (second order) phase transitions shown by dotted and dashed lines, which results in chance probabilities of 10^{-19} (7×10^{-13}), respectively.

The result is consistent with an approximately constant behaviour, despite the fact that there was a factor of 5 difference in the volume. The chance probabilities, that statistical fluctuations changed the dominant behaviour of the volume dependence are negligible. As a conclusion we can say that the staggered QCD transition at $\mu = 0$ is a crossover.

5. The transition temperature

One of the most interesting quantities that can be extracted from lattice simulations is the transition temperature T_c at which hadronic matter is supposed to undergo a transition to a deconfined, quark-gluon phase. This quantity has been vastly debated over the last few years, due to the disagreement on its numerical value observed by different lattice collaborations, which in some cases is as high as 20% of the absolute value. Indeed, the analysis of the HotQCD Collaboration (performed with two different improved staggered fermion actions, asqtad and p4, and with physical strange quark mass and somewhat larger than physical u and d quark masses, $m_s/m_{u,d} = 10$), indicates that the transition region lies in the range of $T = (185\text{--}195)$ MeV. Different observables lead to the same value of T_c [20, 21, 22, 23, 24]. Recent simulations using the p4 action with the quark mass ratio $m_s/m_u = 20$ yielded about 5 MeV shift (towards the smaller values) in the temperature dependence of the studied observables [25]. On the other hand, the re-

sults obtained by our collaboration using the staggered stout action (with physical light and strange quark masses, thus $m_s/m_{u,d} \simeq 28$) are quite different: the value of the transition temperature lies in the range 150–170 MeV, and it changes with the observable used to define it [26, 27]. This is not surprising, since the transition is a cross-over [19]: in this case it is possible to speak about a transition region, in which different observables may have their characteristic points at different temperature values, and the temperature dependences of the various observables play a more important role than any single T_c value. Unfortunately, the 25–30 MeV discrepancy was observed between the two collaborations for the T dependences of the various observables, too.

A lot of effort has been invested, in order to find the origin of the discrepancy between the results of the two collaborations¹. In Refs. [26, 27], we emphasized the role of the proper continuum limit with physical quark masses, showing how the lack of them can distort the result. In [30, 31] we pointed out that the continuum limit can be approached only if one reduces the unphysical pion splitting (the main motivation of our choice of action). From the lattice point of view, we present (for details see [32] our most recent results for several physical quantities: our previous calculations [26, 27] have been extended to an even smaller lattice spacing (down to $a \lesssim 0.075$ fm in the transition region), corresponding to $N_t = 16$. We use physical light and strange quark masses: we fix them by reproducing f_K/m_π and f_K/m_K and by this procedure [27] we get $m_s/m_{u,d} = 28.15$. The HRG model results are obtained both for the physical resonance masses, as listed in the Particle Data Book, and for the distorted spectrum which corresponds to the quark masses and finite lattice spacings of [24]. Our analysis indicates that the discretization effects on hadron masses (and in particular on the nondegenerate, taste-split light pseudoscalar meson masses which emerge as a consequence of the staggered formalism) affect more severely the asqtad and p4 actions than the stout one, in the temperature regime below and around T_c .

In order to illustrate the most important differences between a real phase transition and an analytic cross-over, we recall the water–vapor phase diagram on the temperature *versus* pressure plane (*cf.* [26] and Fig. 4 of the present paper). We study the transition by fixing the pressure to a given value and then varying the temperature. For smaller pressures ($p \lesssim 22$ MPa) there is a first order phase transition. The density jumps, the heat capacity is infinite, and these singular features appear simultaneously, thus exactly at the same critical temperature. At pressure $p \approx 22.064$ MPa and temperature

¹ Note that quite recently preliminary results were presented [28, 29] and the results of the HotQCD Collaboration moved closer to our results. (We include some of these data in our comparisons.)

$T \approx 647.096$ K, there is a critical point with a second order phase transition. This phase transition is also characterized by a singular behaviour².

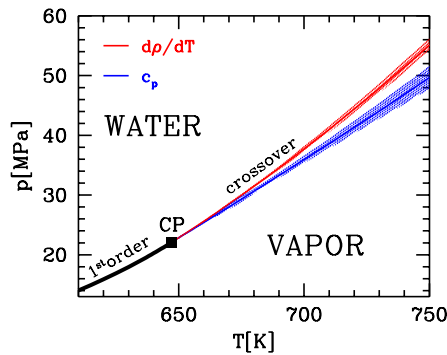


Fig. 4. The phase diagram of water around its critical point (CP). For pressures below the critical value (p_c) the transition is first order, for $p > p_c$ values there is a rapid cross-over. In the cross-over region the critical temperatures defined from different quantities are not necessarily equal. This can be seen for the temperature derivative of the density ($d\rho/dT$) and the specific heat (c_p). The bands show the non-negligible experimental uncertainties (see [35]).

At even larger pressures ($p \gtrsim 22.064$ MPa) the water–vapor transition is an analytic one (the behaviours of various observables are analytic, even in the infinite volume limit). As a consequence, in this pressure region there is no jump in the density when we change the temperature, only a rapid but continuous change. The inflection point of this density–temperature function (the point with the largest, though finite, derivative) can be used to define the pseudocritical temperature (another usual name for it is “transition temperature”) related to the density. Similarly, the heat capacity is always finite, but it has a pronounced peak as we increase the temperature. The position of this peak can be used to define the pseudocritical temperature related to the heat capacity. Despite the fact that there is no singularity, the inflection point and peak position are well defined. The corresponding pseudocritical or transition temperature is usually denoted as T_c .

The most important message here is that the various transition temperatures (*e.g.* those related to the density or heat capacity) behave differently depending on whether we are in the singular (real phase transition) or non-singular (analytic cross-over) region. As it is indicated in the figure, for a real phase transition these critical temperatures coincide, whereas in the

² Note that a real singularity, a phase transition, takes place only in infinite size systems. In our example we have a macroscopic amount of water with $O(10^{23})$ molecules. From the practical point of view, this is an infinitely large system.

non-singular region (for pressures above 22.064 MPa) the pseudocritical temperatures can differ considerably. The fast change (though no jump) in the density is at a lower temperature than the peak in the heat capacity. The transition is a broad cross-over. The pseudocritical temperatures, related to various observables, are separated, but both of them are in the broad transition temperature region. This separation does not mean that we have two transitions (one for the density and one for the heat capacity), it merely reflects the broadness of the transition.

Let us illustrate the situation by increasing the temperature for a pressure of *e.g.* 50 MPa. The density change has its most singular point around 730 K, whereas the heat capacity has its most singular point around 750 K. Physically, we interpret the rapid change in the density as a liberation of the molecules from the liquid phase. The most singular point of the heat capacity corresponds to the remnant of the boiling point of a real first order phase transition. At this point the latent heat indicates the real singularity. At this pressure and at about 740 K one might think to be faced with a state, which has already liberated the molecules but has not boiled yet. This paradox interpretation is not really reasonable, as we said earlier this situation merely reflects the broadness of the transition. Similarly, if we found for QCD the remnant of the confinement transition is at a somewhat higher temperature than the remnant of the chiral transition. It does not mean that we have a phase with chiral symmetry restored with confinement still active. The transition is just a broad one, as found in the previous section.

Now, we present here the temperature dependences with their most singular points for several quantities. We study strange susceptibility, the Polyakov-loop and the chiral condensate, and extract the value of T_c associated to these observables. The T_c values are different which reflects the nature of the crossover transition. For details we refer the reader to Ref. [32].

The strange susceptibility does not need any additional renormalization. The renormalization procedure of the Polyakov loop was given in [27]. The temperature dependences of the strange susceptibility and the Polyakov loop are shown in Fig. 5. The chiral condensate is defined as $\langle \bar{\psi}\psi \rangle_q = T \partial \ln Z / (\partial m_q V)$ for $q = u, d, s$. It is an indicator for the remnant of the chiral transition, since it rapidly changes around T_c . Its renormalization is given in [32]. We also calculate the quantity $\Delta_{l,s}$, which is defined as $[(\bar{\psi}\psi)_{l,T} - m_l/m_s \langle \bar{\psi}\psi \rangle_{s,T}] / [(\bar{\psi}\psi)_{l,0} - m_l/m_s \langle \bar{\psi}\psi \rangle_{s,0}]$ for $l = u, d$. Since the results at different lattice spacings are essentially on top of each other, we connect them to lead the eye (see Fig. 6). The value of T_c that we obtain from the inflection point of the latter observable is $T_c = 157(3)(3)$.

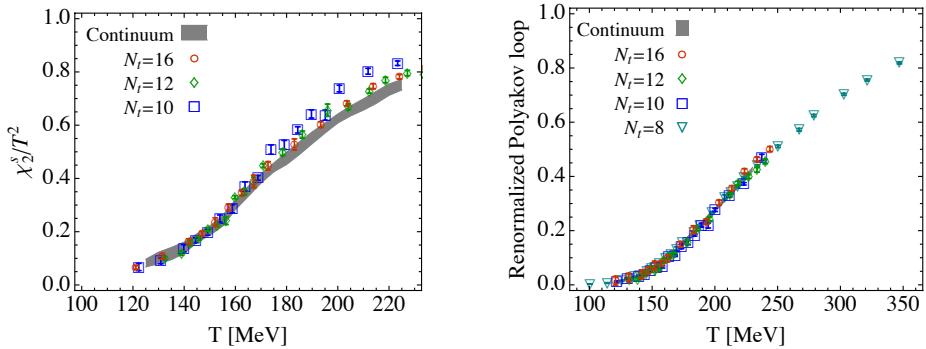


Fig. 5. Left: strange quark number susceptibility as a function of the temperature. Right: renormalized Polyakov loop as a function of the temperature. In both figures, the different symbols correspond to different N_t . The gray band is the continuum extrapolated result.

It is also instructive to compare the present results obtained on $N_t = 6, 8, 10, 12$ and 16 with the results of the HotQCD Collaboration (*cf.* [32]). Figure 6 shows this comparison, too. As it can be seen, the results of the HotQCD Collaboration are getting closer and closer to our predictions. The long standing discrepancy is disappearing.

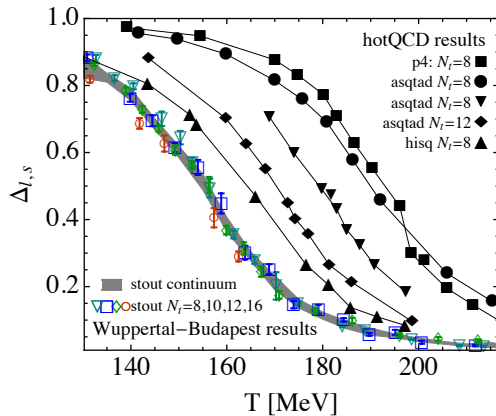


Fig. 6. The subtracted chiral condensate $\Delta_{l,s}$ as a function of the temperature. We show a comparison between stout, asqtad, p4 and HISQ [24,29] results. Our results are shown by (coloured) open symbols, whereas the hotQCD results are shown by full black symbols. The gray band is our continuum result, the thin lines for the hotQCD data are intended to lead the eye. Our stout results were all obtained by the physical pion mass of 135 MeV. The full dots and squares correspond to $m_\pi = 220$ MeV, the full triangles and diamonds correspond to $m_\pi = 160$ MeV of the HotQCD Collaboration.

6. QCD equation of state

Next, we present our results regarding the equation of state. The details of this calculation can be found in [33]. It is important to emphasize that quark masses were set to their physical values and we used quite fine lattices upto $N_t = 12$. We have explicitly showed that for our systems the finite volume corrections are under control. The left panel of Fig. 7 shows two systems. One of them with a volume V the other one with a volume of $8V$. As it can be seen for the whole temperature range, there are practically no finite volume corrections, the two curves are lying on top of each other. The right panel shows the continuum limits at three representative temperatures based on simulations upto temporal extension of 12. In Fig. 8 the T dependence of the trace anomaly is shown for the 2+1 flavour system. We have results at four different lattice spacings. Results show essentially no dependence on a , they all lie on top of each other. Only the coarsest $N_t = 6$ lattice shows some deviation around ~ 300 MeV. In the same figure, we zoom in to the transition region. Here we also show the results from the Hadron Resonance Gas model: a good agreement with the lattice results is found up to $T \sim 140$ MeV.

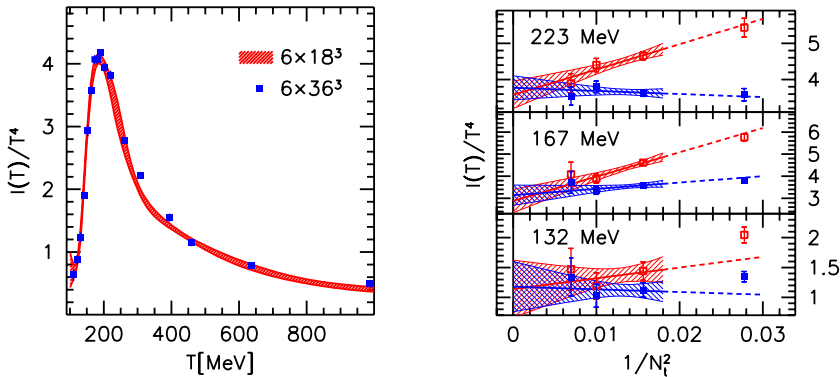


Fig. 7. Left: the trace anomaly on lattices with different spatial volumes: $N_s/N_t = 3$ (grey (red) band) and $N_s/N_t = 6$ (blue points). Right: the trace anomaly at three different temperatures as a function of $1/N_t^2$. Filled (blue) symbols represent the results within the lattice tree-level improvement framework, (red) opened symbols show the results without this improvement. The error of the continuum extrapolated value is about 0.4 for all three temperatures.

In order to obtain the pressure, we determine its partial derivatives with respect to the bare lattice parameters. p is then rewritten as a multidimensional integral along a path in the space of bare parameters. The result is shown in Fig. 9. To obtain the EoS for various m_π , we simulate for a wide range of bare parameters on the plane of $m_{u,d}$ and β (m_s is fixed to its phys-

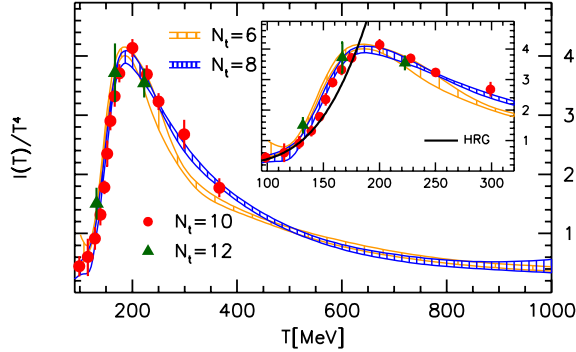


Fig. 8. The trace anomaly $I = \epsilon - 3p$ normalized by T^4 as a function of the temperature on $N_t = 6, 8, 10$ and 12 lattices.

ical value). Having obtained this large set of data we generalize the integral method and include all possible integration paths into the analysis [33, 34]. We remove the additive divergence of p by subtracting the same observables measured on a lattice, with the same bare parameters but at a different T value. Here we use lattices with a large enough temporal extent, so it can be regarded as $T = 0$.

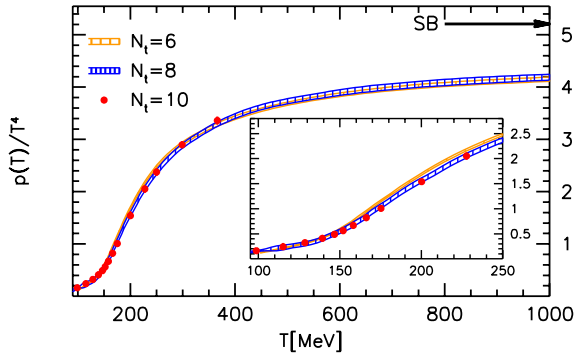


Fig. 9. The pressure normalized by T^4 as a function of the temperature on $N_t = 6, 8$ and 10 lattices. The Stefan–Boltzmann limit $p_{\text{SB}}(T) \approx 5.209 T^4$ is indicated by an arrow. For our highest temperature $T = 1000$ MeV the pressure is almost 20% below this limit.

It is also instructive to compare the present results obtained on $N_t = 6, 8, 10$ and 12 with the results of the HotQCD Collaboration (*cf.* [32]). Figure 10 shows this comparison for the trace anomaly. As it can be seen the results of the HotQCD Collaboration are still quite far away from our results. Their peak position is about at a 20 MeV higher temperature, whereas their peak heights are about 50% larger than in our. The clarification of this discrepancy remains for the future.

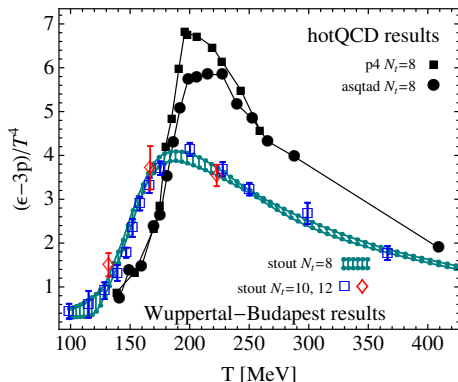


Fig. 10. The normalized trace anomaly obtained in our study is compared to recent results from the HotQCD Collaboration [24, 25].

REFERENCES

- [1] J. Kuti, J. Polonyi, K. Szlachanyi, *Phys. Lett.* **B98**, 199 (1981).
- [2] L.D. McLerran, B. Svetitsky, *Phys. Lett.* **B98**, 195 (1981).
- [3] T. Celik, J. Engels, H. Satz, *Phys. Lett.* **B125**, 411 (1983).
- [4] J.B. Kogut *et al.*, *Phys. Rev. Lett.* **50**, 393 (1983).
- [5] S.A. Gottlieb *et al.*, *Phys. Rev. Lett.* **55**, 1958 (1985).
- [6] F.R. Brown *et al.*, *Phys. Rev. Lett.* **61**, 2058 (1988).
- [7] M. Fukugita, M. Okawa, A. Ukawa, *Phys. Rev. Lett.* **63**, 1768 (1989).
- [8] S. Durr *et al.*, *Science* **322**, 1224 (2008) [arXiv:0906.3599v1 [hep-lat]].
- [9] R.D. Pisarski, F. Wilczek, *Phys. Rev.* **D29**, 338 (1984).
- [10] Z. Fodor, S.D. Katz, *Phys. Lett.* **B534**, 87 (2002) [arXiv:hep-lat/0104001].
- [11] Z. Fodor, S.D. Katz, *J. High Energy Phys.* **03**, 014 (2002) [arXiv:hep-lat/0106002].
- [12] Z. Fodor, S. Katz, *Landolt-Boernstein*, vol. 1-23A, Springer-Verlag, Berlin Heidelberg 2010, pp. 2–27 [arXiv:0908.3341v1 [hep-ph]].
- [13] Z. Fodor, S.D. Katz, *J. High Energy Phys.* **04**, 050 (2004) [arXiv:hep-lat/0402006].
- [14] G. Endrodi, Z. Fodor, S. Katz, K. Szabo, *J. High Energy Phys.* **1104**, 001 (2011) [arXiv:1102.1356v1 [hep-lat]].
- [15] I. Montvay, G. Munster, *Quantum Fields on a Lattice*, Cambridge, UK: Univ. Pr., 1994, 491 p. (Cambridge monographs on mathematical physics).
- [16] D.J. Schwarz, *Ann. Phys.* **12**, 220 (2003) [arXiv:astro-ph/0303574].
- [17] E. Witten, *Phys. Rev.* **D30**, 272 (1984).
- [18] J.H. Applegate, C.J. Hogan, *Phys. Rev.* **D31**, 3037 (1985).
- [19] Y. Aoki *et al.*, *Nature* **443**, 675 (2006) [arXiv:hep-lat/0611014].

- [20] M. Cheng *et al.*, *Phys. Rev.* **D74**, 054507 (2006) [arXiv:hep-lat/0608013].
- [21] [HotQCD Collaboration] C.E. Detar, R. Gupta, *PoS LAT2007*, 179 (2007) [arXiv:0710.1655v1 [hep-lat]].
- [22] F. Karsch, *PoS LAT2007*, 015 (2007) [arXiv:0711.0661v1 [hep-lat]].
- [23] [RBC Collaboration] F. Karsch, *J. Phys. G* **35**, 104096 (2008) [arXiv:0804.4148v1 [hep-lat]].
- [24] A. Bazavov *et al.*, *Phys. Rev.* **D80**, 014504 (2009) [arXiv:0903.4379v1 [hep-lat]].
- [25] M. Cheng *et al.*, *Phys. Rev.* **D81**, 054504 (2010) [arXiv:0911.2215v2 [hep-lat]].
- [26] Y. Aoki, Z. Fodor, S.D. Katz, K.K. Szabo, *Phys. Lett.* **B643**, 46 (2006) [arXiv:hep-lat/0609068].
- [27] Y. Aoki *et al.*, *J. High Energy Phys.* **06**, 088 (2009) [arXiv:0903.4155v1 [hep-lat]].
- [28] [HotQCD Collaboration] A. Bazavov, P. Petreczky, *PoS LAT2009*, 163 (2009) [arXiv:0912.5421v1 [hep-lat]].
- [29] [HotQCD Collaboration] A. Bazavov, P. Petreczky, *J. Phys. Conf. Ser.* **230**, 012014 (2010) [arXiv:1005.1131v1 [hep-lat]].
- [30] Y. Aoki, Z. Fodor, S.D. Katz, K.K. Szabo, *J. High Energy Phys.* **01**, 089 (2006) [arXiv:hep-lat/0510084].
- [31] Z. Fodor, *PoS LAT2007*, 011 (2007) [arXiv:0711.0336v1 [hep-lat]].
- [32] [Wuppertal–Budapest Collaboration] S. Borsanyi *et al.*, *J. High Energy Phys.* **1009**, 073 (2010) [arXiv:1005.3508v1 [hep-lat]].
- [33] S. Borsanyi *et al.*, *J. High Energy Phys.* **1011**, 077 (2010) [arXiv:1007.2580v2 [hep-lat]].
- [34] G. Endrodi, *Comput. Phys. Commun.* **182**, 1307 (2011) [arXiv:1010.2952v2 [physics.comp-ph]].
- [35] B. Spang, <http://www.cheresources.com/iapwsif97.shtml>